JACS
JOURNAL OF THE AMERICAN CHEMICAL SOCIETY
Communication
pubs.acs.org/JACS

All-Atom Molecular Dynamics Simulation of Photosystem II Embedded in Thylakoid Membrane

Koji Ogata,[†] Taichi Yuki,[‡] Makoto Hatakeyama,[†] Waka Uchida,[‡] and Shinichiro Nakamura*[,†]

[†]Nakamura Laboratory, RIKEN Innovation Center, 2-1 Hirosawa, Wako, Saitama 351-0198, Japan

[‡]Department of Biomolecular Engineering, Tokyo Institute of Technology, 4259 Nagatsuta, Midori-ku, Yokohama 226-8503, Japan

Supporting Information

ABSTRACT: The molecular dynamics simulation is reported. The latest data on photosystem II structure, a thylakoid membrane model with the same lipid class distribution and fatty acid composition as the native thylakoid membrane, are used. The results indicate that the transfer of water, oxygen and protons has different pathways. The root mean square (rms)-fluctuation analysis of trajectory revealed that the residues surrounding the oxygen-evolving center (OEC) show small fluctuations and that most of the water molecules there show large fluctuation and are on proposed pathways for water and oxygen transfer. The water molecules near the OEC having small fluctuation could be involved in proton transfer. We assume that each kind of pathway characterized in this study plays a role in photosynthesis.

Photosystem II (PSII) is a transmembrane protein−cofactor complex governing the initial photosynthetic process in plants, algae, and cyanobacteria. It consists of about 20 protein subunits, several quinones, and a system of chlorophyll and carotenoid pigments.[1] Its structure, resolved using X-ray crystallography techniques,[2] is available from the Protein Data Bank (PDB).[3] The high-resolution structure of *Thermosynechococcus vulcanus* PSII (PDB ID: 3ARC) obtained in 2011 by Umena et al.[2c] clearly identifies the positions of atoms in the oxygen-evolving center (OEC) and in residues contacting the OEC. These are important clues to the mechanism of water oxidation, and by combining the experimental evidence, such as spectroscopic analyses,[4] it guides us to elucidate the mechanism of photosynthesis.

Molecular dynamics (MD) simulation is a powerful tool in the study of dynamic features of biomolecules such as proteins, DNA, and sugar chains,[5] and MD simulations of PSII have been reported by several groups. Bruce and his colleagues, for example, have used MD simulations with monomeric PSII to identify the channels along which water moves from outside PSII to the OEC.[6] They visualized the water molecules moving in the channels.

To clarify the dynamics of the S_1 state of the OEC, in this paper we report all-atom MD simulation of monomeric and dimeric PSII complexes embedded in the thylakoid membrane. Focusing on the effects of electric fields generated by surrounding residues that assist oxygen evolution, we clarify the water pathways that reflect these effects.

The initial structure is critical if MD simulations are to reproduce the biological events taking place in the native state. We therefore used the latest structure of dimeric PSII embedded in the thylakoid membrane and used a model membrane whose lipid composition and fatty acid distribution were the same as those of the native membrane. In general, the lipid composition in thylakoid membrane reflects the circumstances, such as lifetime, temperature, etc.[7] We used the lipid composition reported by Sakurai et al.,[8] which is regarded as the standard lipid composition of the thylakoid membrane in *T. vulcanus*. The complete structure for entire amino acid sequence of PSII was generated by assigning coordinates to the atoms missing in the original PDB file. The modeling of PSII and the thylakoid membrane is described in detail in the Supporting Information (SI). The PSII with the thylakoid membrane was solvated in water boxes (275 Å × 195 Å × 220 Å) containing more than 300 000 TIP3P water molecules. The water molecules were located at both of lumen and stroma sides (Figure S1). The simulation was performed in 10 ns in total, with 2.0 fs time step (see SI), and we analyzed the trajectory after the equilibrium state, ranging from 2 to 10 ns.

From the trajectory of the simulation, we confirmed that the PSII-with-thylakoid-membrane system reaches the equilibrium state because the Cα-rmsd (root mean square deviation) values demonstrated to be almost constant (Figure S2). Figure 1 shows a typical snapshot of the dimeric structure of the PSII embedded in the thylakoid membrane. The structures of the two monomer PSIIs and their interfaces are roughly the same. Symmetry is of course not imposed in the simulation; nevertheless, the rmsd of chain A and chain B is so small that we cannot argue the different conformations (Figure S3). This suggests that our initial model structure based on the high-resolution X-ray data of PSII dimer with the thylakoid membrane is close to the native state and so reliable that the performed simulation is reasonable.

PSII is well packed with the lipids in thylakoid membrane, and the membrane model we used contained 544 MGDG molecules, 331 DGDG molecules, 339 SQDG molecules, and 46 PG molecules. These numbers are consistent with cyanobacteria's lipid class composition.[8] The four lipid classes are randomly distributed and no specific lipid class interacts with PSII proteins (Figure 1a). The helixes in the transmembrane region in the PSII are completely embedded in the thylakoid membrane, and intertwining fatty acids of the lipids in

Received: May 1, 2013
Published: October 9, 2013

dx.doi.org/10.1021/ja404317d | J. Am. Chem. Soc. 2013, 135, 15670−15673

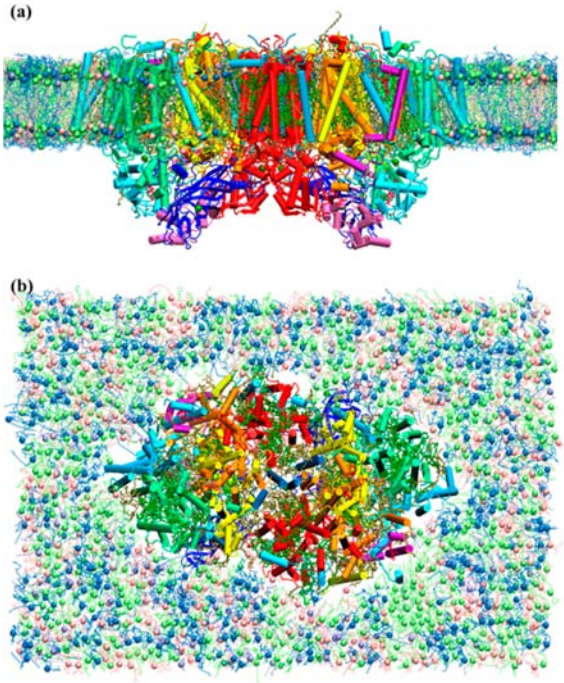

Figure 1. Typical snapshot of PSII embeded in the thylakoid membrane: (a) side view and (b) view from the lumenal side. The PSII is shown by a New Cartoon drawing, cofactors are drawn by line models, and the membrane lipids and branched-carbon in those lipids are shown by line and vdW models, respectively. The chains in PSII were colored as follows: A, Y, a, y, yellow; B, b, red; C, c, green; D, J, L, d, j, l, orange; E, e, purple; F, H, I, K, V, Y, Z, f, h, i, k, v, y, z, cyan; M, O, T, m, o, t, blue; U, u, mauve. MGDG is shown in lime, DGDG in blue, SQDG in gray, and PG in pink.

the thylakoid membrane are packed with each other. The thylakoid membrane of cyanobacteria contains many unsaturated fatty acids (Table S1) in which most of the unsaturated bonds take the form of cis configurations. Unlike trans fatty acids, in which most of the bonds are saturated, these cis fatty acids are unable to form a straight shape. Therefore, they induce the entanglement that makes the entire structure stable. This may be an important function of the unsaturated fatty acids in the thylakoid membrane.

Lipids in the thylakoid membrane distinctly showed a large movement during the simulation. To visualize this, we projected the trajectories of lipids onto *XY* plane. The 2D Brownian-like motion of the lipid diffusion is shown in Figure 2. The average of the self-diffusion coefficient for all the lipids is 3.0×10^{-8} (cm^2/s). It is the same order of magnitude with single lipid of 1,2-dipalmitoyl-*sn*-glycero-3-phosphocholine (DPPC).[9] The range of the diffusion in either the *X* or *Y* direction is around 6 Å. This value is independent of the lipid class, fatty acid length, or number of unsaturated bonds. Moreover, each lipid has the large internal conformational changes, in which the average rmsd of MGDG, DGDG, SQDG, and PG for initial structure are 3.9, 3.9, 3.6, and 3.8 Å, respectively. These values indicate that the lipid freely moved with the conformational changes during the simulation. The protein diffusion range, in contrast, is much smaller than that of lipids: the maximum movements along the *X* and *Y* directions are 1.9 and 3.0 Å, respectively (Figure S4). And the self-diffusion coefficient for all the lipids is 3.6×10^{-9} (cm^2/s). This value is 1 order of magnitude smaller than that of the average of all the lipids. The current simulation reproduces the fluid phase

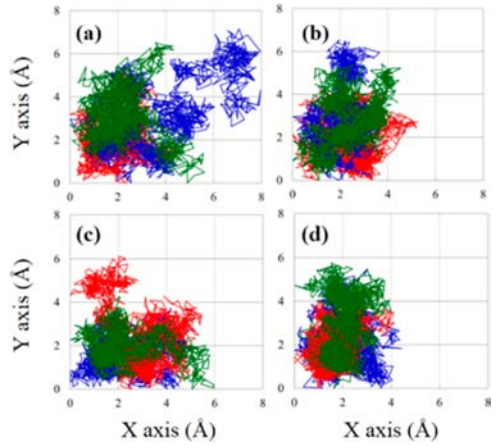

Figure 2. Trajectories of lipid diffusion (mass center projected onto the *xy* plane): (a) MGDG, (b) DGDG (c) SQDG, and (d) PG. Three lipids in each headgroup are randomly selected from thylakoid membrane lipid molecules and colored in blue, red, and green.

models of the lipids in the thylakoid membrane and shows that the dimeric PSII has small movement in the fluid-phase thylakoid membrane. The grana thylakoid membrane contains high density of protein complexes, which occupy about 80%.[10] This dense structure may prevent the free movement of PSII in the thylakoid membrane. Therefore, PSII protein appears immobile in the thylakoid membrane in low light conditions without photoinhibition,[11] and PSII shows lower mobility than lipids in the thylakoid membrane. These results are consistent with those experimentally obtained when the mobility of PSII protein in the thylakoid membrane was investigated.[10,11] In our simulation, the interaction of the other proteins such as light harvesting chlorophyll–protein complex (LHC II) or phycobilisome in cyanobacteria, red alga, and glaucophytes was not considered. Still, the mobility of the protein and lipids are comparatively similar to the experimental data.[10,11] Therefore, we consider that the dynamics of PSII and thylakoid membrane demonstrates the similar behavior with the native structure.

Fluctuation analysis (see SI) was applied to the trajectory of the simulation. Many residues surrounding the OEC showed small fluctuation throughout the MD simulation. Most of these residues were in the subunits of PSII, whose amino acid sequences are well-conserved in different organisms.[12] Residues showing large fluctuation, on the other hand, were located at the surface area of the PSII as shown in Figure 3. The number of residues with large fluctuation was smaller than that with small fluctuation. The residues with large fluctuation interacted with each other and were influenced by the bulk water molecules. Most of these residues were in the PsbO subunit. The simulation trajectory showed that the dynamics of PsbO subunit are characterized by large movement. Since the structure of PsbO is completely exposed on the lumen side of the membrane, it is natural that this subunit showed large movement due to the influence of water molecules and all the other PSII subunits.

Most of the water molecules in PSII crystal structure moved with large fluctuation during the simulation. Water molecules, unlike the residues in proteins, can move freely during the simulation because they do not have covalent bonds with other molecules. Some of the water molecules near the OEC, however, showed different behavior: a considerable number showed small fluctuations. These are the ones in channels (i.e.,

dx.doi.org/10.1021/ja404317d | J. Am. Chem. Soc. 2013, 135, 15670–15673

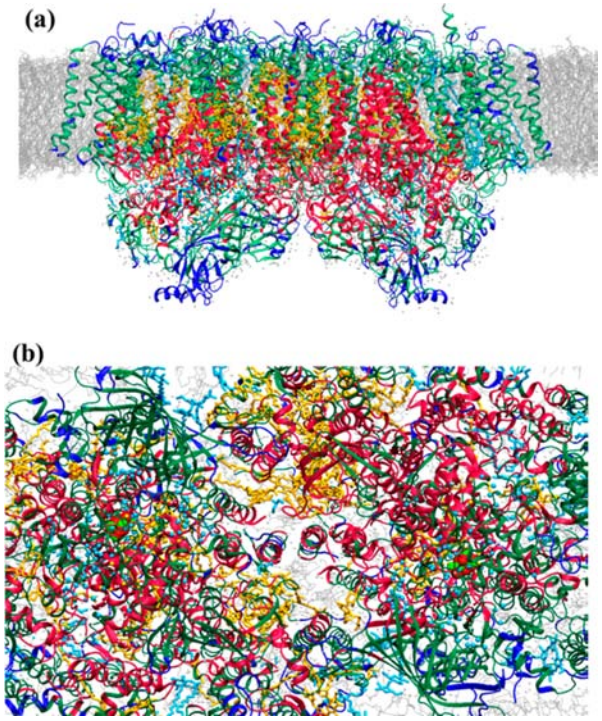

Figure 3. Rms-fluctuation of PSII and water molecules: (a) side view and (b) view from the thylakoid-lumen side. Residues with small and large fluctuation are shown in red and blue, respectively; the other residues are shown in green. Water molecules and ligands with small and large fluctuation are shown in yellow and cyan, respectively; the others are shown in gray. The OEC is shown by a CPK model and thylakoid membrane is shown by a line model colored gray.

on pathways), and we analyzed the rms-fluctuation of water molecules precisely so that we locate the water transfer pathways, as mentioned below. MD trajectory revealed that some were trapped and could not enter or leave the PSII. All the waters in crystal structure near the OEC kept their positions and did not move out of the complex. Our simulation was of the S_1 state and there was no change at the MnCa cluster (no O_2 was leaving) in the center of the OEC. The PSII interior near the OEC seems to be so packed with water, ions, and cofactors that there is no space to move freely. However, the number of waters within 6 Å from OEC is fluctuated during the simulation (Figure S4). Therefore, we can infer that the waters were shifted and filled the cavities and moved out from the cavities near OEC. These motions will give a chance to change the position of waters. Furthermore, our simulation is too short a time scale to change the water position in the tight space. Therefore, by increasing time scale, we will be able to observe the water that change their position and move out of the complex.

In our simulation, three pathways were detected. Along the pathways, many bulk water molecules were entering and leaving the PSII complex (Videos S2,S3). Although similar pathways were shown in previous reports (not with simulation) by analyzing hydrogen network among waters and surrounding residues, calculating the cavities and the convex hulls in the static structure,[2c,13] also (combination with simulation on partial protein) by performing pK_a calculation or by observing the waters and surrounding the residues, previous reports suggested that the pathways globally for water, oxygen, or proton transfer.[14] We here present detailed property and function for each pathway by the MD trajectory. The waters behaviors are traced from OEC to the surface of PSII (Figure 4

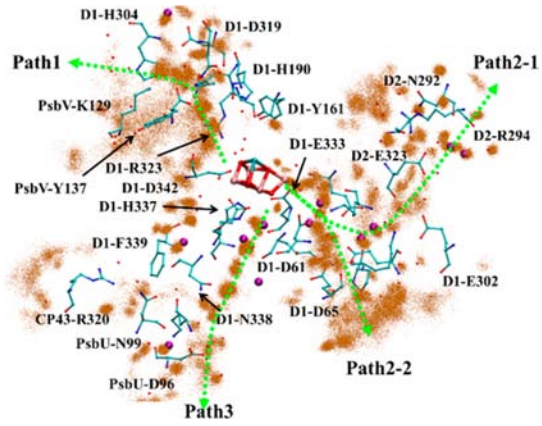

Figure 4. Pathways for water, oxygen and proton transfer. Arrows colored in green are predictive pathways. Waters with small fluctuation are colored in purple. And the water distribution, which was generated by all the waters having the distance within 5 Å from the residues consisting of the channels in all the trajectories, are colored in brown.

and Figure S6). The pathways marked Path1 and Path2 are contained waters and charged residues, (but not Path3, to be discussed later). For the sake of comparison, the assignment of current water pathways to the previously reported channels are shown in Table 1.

Table 1. Assignment of Current Water Pathways to Previously Reported Channels[a]

This work	Path1	Path2	Path3
Murray and Barber[13b]	(i)	(iii)	-
Ho and Styring[13a]	("Back")	-	"Narrow"
Gabdulkhakov et al.[13c]	(A1,A2)	(C)	(E, F)
Vassiliev et al.[14b]	(5)	(1)	2
Umena et al.[2c]	Figure 3b	Figure 4b	Figure 4c

[a]When previously reported pathways are only partially overlapping with current ones, they are shown in parentheses.

The pathway marked Path1 shows a hydrogen network starting from D1-Y161 to PsbV-K129. Between these residues, many waters were occupied and broadly distributed during the simulation. The number of waters with small fluctuation, which is convenient for the proton transfer, are very small in this pathway. Entering and leaving water molecules from PSII were observed near PsbV-K129. The pathway marked Path2 shows the hydrogen network starting from D1-D61 to CP47-A361.[2c] This pathway branches into two pathways, and we marked these pathways as Path2-1 and Path2-2. We can see the waters molecules with small fluctuation in the pathway marked Path2-1. According to the previous reports,[13a,b] the pathway marked Path2-1 is suggested as proton exit channel. Our results agree with this suggestion for the pathway marked Path2-1. On the other hand, many entering and leaving water molecules are observed near D1-E65 and D2-E312 (Videos S2,S3), which is terminal of the pathway marked Path2-2. The length of this pathway is very short from OEC in comparison with other pathways. Therefore, the short distance is favorable for water molecules to enter, also for O2 molecules to leave via this pathway.

dx.doi.org/10.1021/ja404317d | J. Am. Chem. Soc. 2013, 135, 15670−15673

The pathway marked Path3, starting from O4 in OEC (PDB based atom name) and terminated at PsbU-D96, contained mainly waters. There are no waters with small fluctuation at the middle of the pathway. This feature is similar to that of the pathway marked Path1. Although it is not easy to see entering and leaving water molecules from this pathway, in condition that we should be cautious about our limited period of simulation, we infer that this Path3 does work for entering waters or exiting oxygen molecules. (Notice that we see in Videos S2,S3, near the pathway marked Path3, many waters entering and leaving from the convex hull; it is not the path that penetrates from OEC to surface.)

These results indicate that the proton transfer along the pathway marked Path2-1 is efficient because there are many water molecules staying on the path (i.e., proton hopping is efficient). On the other hand, the pathways marked Path1, Path2-2 and Path3 are suitable for the transfer of molecules (H_2O, H_3O^+, and O_2) toward the surface of PSII because waters need to change their location for eliminating H_3O^+ and O_2.

The results of MD simulation thus show that the pathways marked Path1, Path2-2 and Path3 are efficient channel for water and oxygen molecules. The detected pathways marked Path1, Path2-1 and Path3 are consistent with the hydrogen network analysis by Umena at al.[2c] The property and function of the pathway marked Path2-2 are newly found by the current MD simulation. These results suggest that the pathways of water, oxygen, and proton transfer are different from each other, reflecting the dynamic properties of ions or molecules.

We performed a MD simulation using a thylakoid membrane model having a lipid class composition and fatty acid distribution the same as those of the native membrane, PSII dimers with full cofactors and without any constraints on PSII. The residues surrounding OEC did not show large movement during the simulation, whereas the water molecules did. The water molecules showing small fluctuation were functionally gathered in water, oxygen, and proton channels. This study suggests that each of these three pathways plays an important role in photosynthesis.

■ ASSOCIATED CONTENT

Ⓢ Supporting Information

Supporting tables and figures and a description of all calculation procedures. This material is available free of charge via the Internet at http://pubs.acs.org.

■ AUTHOR INFORMATION

Corresponding Author

snakamura@riken.jp

Notes

The authors declare no competing financial interest.

■ ACKNOWLEDGMENTS

We thank the KAITEKI Institute (Mitsubishi Chemical Holdings) for support, Dr. J. R. Shen and Dr. S. Yokojima for fruitful discussions, and Dr. Massimo Marchi at the Commissariat à l'Energie Atomique for kindly giving us a file of the parameter sets on chlorophyll A. All calculations in this study were performed using the RIKEN Integrated Cluster of Clusters (RICC) facility.

■ REFERENCES

(1) Wydrzynski, T.; Satoh, K. *Photosystem II: The Light-Driven Water: Plastoquinone Oxidoreductase*; Springer: Dordrecht, The Netherlands, 2006; Vol. *22*.

(2) (a) Broser, M.; Glockner, C.; Gabdulkhakov, A.; et al. *J. Biol. Chem.* **2011**, *286* (18), 15964−72. (b) Guskov, A.; Kern, J.; Gabdulkhakov, A.; Broser, M.; Zouni, A.; Saenger, W. *Nat. Struct. Mol. Biol.* **2009**, *16* (3), 334−42. (c) Umena, Y.; Kawakami, K.; Shen, J. R.; Kamiya, N. *Nature* **2011**, *473* (7345), 55−60. (d) Loll, B.; Kern, J.; Saenger, W.; Zouni, A.; Biesiadka, J. *Nature* **2005**, *438* (7070), 1040−4.

(3) Berman, H. M.; Westbrook, J.; Feng, Z.; Gilliland, G.; Bhat, T. N.; Weissig, H.; Shindyalov, I. N.; Bourne, P. E. *Nucleic Acids Res.* **2000**, *28* (1), 235−42.

(4) (a) Sauer, K.; Yano, J.; Yachandra, V. K. *Coord. Chem. Rev.* **2008**, *252* (3−4), 318−35. (b) Yano, J.; Yachandra, V. K. *Inorg. Chem.* **2008**, *47* (6), 1711−26. (c) Yano, J.; Kern, J.; Sauer, K.; et al. *Science* **2006**, *314* (5800), 821−5.

(5) (a) Case, D. A.; Cheatham, T. E., III; Darden, T.; et al. *J. Comput. Chem.* **2005**, *26* (16), 1668−88. (b) Brooks, B. R.; Brooks, C. L., III; Mackerell, A. D., Jr.; et al. *J. Comput. Chem.* **2009**, *30* (10), 1545−614. (c) Van Der Spoel, D.; Lindahl, E.; Hess, B.; Groenhof, G.; Mark, A. E.; Berendsen, H. J. *J. Comput. Chem.* **2005**, *26* (16), 1701−18.

(6) (a) Vasil'ev, S.; Bruce, D. *Biophys. J.* **2006**, *90* (9), 3062−73. (b) Vassiliev, S.; Bruce, D. *Photosynth. Res.* **2008**, *97* (1), 75−89. (c) Vassiliev, S.; Comte, P.; Mahboob, A.; Bruce, D. *Biochemistry* **2010**, *49* (9), 1873−81.

(7) (a) Kiseleva, L. L.; Horvàth, I.; Vigh, L.; Los, D. A. *FEMS Microbiol. Lett.* **1999**, *175* (2), 179−83. (b) Chapman, D. J.; De-Felice, J.; Barber, J. *Plant Physiol.* **1983**, *72* (1), 225−8.

(8) Sakurai, I.; Shen, J. R.; Leng, J.; Ohashi, S.; Kobayashi, M.; Wada, H. *J. Biochem.* **2006**, *140* (2), 201−9.

(9) Devaux, P.; McConnell, H. *J. Am. Chem. Soc.* **1972**, *94* (13), 4475−81.

(10) (a) Kirchhoff, H.; Mukherjee, U.; Galla, H. J. *Biochemistry* **2002**, *41* (15), 4872−82. (b) Kirchhoff, H.; Lenhert, S.; Buchel, C.; Chi, L.; Nield, J. *Biochemistry* **2008**, *47* (1), 431−40.

(11) (a) Mullineaux, C. W.; Tobin, M. J.; Jones, G. R. *Nature* **1997**, *390* (6658), 421−4. (b) Mullineaux, C. W.; Sarcina, M. *Trends Plant Sci.* **2002**, *7* (6), 237−40. (c) Goral, T. K.; Johnson, M. P.; Brain, A. P.; Kirchhoff, H.; Ruban, A. V.; Mullineaux, C. W. *Plant J.* **2010**, *62* (6), 948−59. (d) Sarcina, M.; Bouzovitis, N.; Mullineaux, C. W. *Plant Cell* **2006**, *18* (2), 457−64.

(12) Enami, I.; Okumura, A.; Nagao, R.; Suzuki, T.; Iwai, M.; Shen, J. R. *Photosynth. Res.* **2008**, *98* (1−3), 349−63.

(13) (a) Ho, F. M.; Styring, S. *Biochim. Biophys. Acta, Bioenerg.* **2008**, *1777* (2), 140−53. (b) Murray, J. W.; Barber, J. *J. Struct. Biol.* **2007**, *159* (2), 228−37. (c) Gabdulkhakov, A.; Guskov, A.; Broser, M.; Kern, J.; Muh, F.; Saenger, W.; Zouni, A. *Structure* **2009**, *17* (9), 1223−34.

(14) (a) Ishikita, H.; Saenger, W.; Loll, B.; Biesiadka, J.; Knapp, E.-W. *Biochemistry* **2006**, *45* (7), 2063−71. (b) Vassiliev, S.; Zaraiskaya, T.; Bruce, D. *Biochim. Biophys. Acta* **2012**, *1817* (9), 1671−8.